

## New Flow Dissipation Mechanisms in Superfluid $^3\text{He}$

R. W. Simmonds, A. Marchenkov, S. Vitale,\* J. C. Davis, and R. E. Packard

*Physics Department, University of California, Berkeley, California 94720*

(Received 1 March 2000)

We have studied the flow of superfluid  $^3\text{He}$ -B forced through small apertures. There are unexpectedly large dissipative currents, which can be described by two independent processes. One process involves the creation of quasiparticles within the aperture and their subsequent acceleration in the ambient pressure gradient. The second process involves the dissipative precession of a texture in a geometry-induced anisotropic order parameter. For both mechanisms we make a simple estimate of the relevant effect and find these agree well with the data.

PACS numbers: 67.57.De, 67.57.Fg, 67.57.Hi, 74.50.+r

How can a flowing superfluid (charged or neutral) dissipate kinetic energy without ordinary viscous processes? This intriguing question has long been discussed and has led to the idea of energy dissipation due to phase unwinding or slippage, arising from the motion of quantized vortices [1] or other textural singularities. Here we report experimental evidence for two other sources of superfluid dissipation which occur when superfluid  $^3\text{He}$  is forced through a small aperture. In particular, we suggest that the usual phase slippage mechanisms are accompanied by an additional new phenomenon associated with the creation of quasiparticles within the weak link and their subsequent transport by a pressure gradient. Elements of this phenomenological model are present in theories describing nonlinear currents in superconducting weak links [2]. We find this model quantitatively describes dissipative currents, proportional to the square root of the pressure head, which seem to be a general feature of forced  $^3\text{He}$  superflow.

Our experiment consists of determining the family of characteristic mass current vs pressure ( $I$ - $P$ ) curves for a superfluid  $^3\text{He}$  weak link [3,4] (a  $65 \times 65$  array of nominally 100 nm diameter apertures placed in a nominally 50 nm thick membrane). Such curves are analogous to the current-voltage ( $I$ - $V$ ) curves for superconducting Josephson weak links. To perform these measurements we use a modified version of our flow cell described previously [3,5]. We have developed an electromechanical feedback technique, which permits us to drive mass current through the weak link at constant pressure head [6] (i.e., pressure biased). The pressure scale is determined from an *in situ* calibration based on the Josephson frequency relation [3]. The mass current is determined by monitoring the motion of a flexible diaphragm.

Figure 1 shows the family of  $I$ - $P$  curves for various temperatures. There are two families of curves because, as predicted by theory [8] and seen experimentally [4], the weak link array has the property of being able to exist in two different configurations, each having a distinct current-phase relation  $I(\phi)$ . We refer to the two configurations as the  $H$  and  $L$  states, which have high and low critical currents, respectively [ $I_c^H(T) = (124 \pm 9) \times$

$$(1 - T/T_c)^{1.51 \pm 0.04} \text{ ng/s}, \quad I_c^L(T) = (57 \pm 4)(1 - T/T_c)^{1.87 \pm 0.06} \text{ ng/s}].$$

Consideration of a voltage biased superconducting weak link would suggest that one might simply expect the superfluid  $^3\text{He}$   $I$ - $P$  curves to be linear and extrapolating to  $P = 0$ , with a slope determined by the *normal fluid conductance*. However, we have directly measured the normal fluid currents just above  $T_c$  and find they are *3 orders of magnitude* smaller than the currents shown in Fig. 1. In addition the measured curves below  $T_c$  are not linear, showing obvious curvature, pronounced at low pressures. Furthermore, as Fig. 1 shows, the currents *increase* as the temperature *decreases*. Thus, it seems that these currents are associated with the increasing superfluid order parameter.

We find that for both  $H$  and  $L$  states, the curves are well fit to the functional form

$$I = I_1 + I_2 = G_1 P + G_2 \sqrt{P}, \quad (1)$$

where  $G_1$  and  $G_2$  are fit parameters. The solid lines drawn through the data in Fig. 1 demonstrate the quality of the fit (see, in particular, the  $L$ -state inset), which is good for all the curves. From the form of (1),  $G_1$  and  $G_2$  can be considered as linear and nonlinear conductances, respectively. These conductances effectively form two parallel shunts across the ideal weak link. The shunts generate two types of dc currents,  $I_1$  and  $I_2$ , which we suggest arise from two distinctly different mechanisms. As we show below, the linear current  $I_1$  can be understood in terms of orbital dissipation due to a precessing texture.

We focus first on a phenomenological model, depicted in Fig. 2, which explains the origin of the nonlinear current,  $I_2$ , and quantitatively predicts the magnitude of  $G_2$ . The thread of the argument has several pieces: (i) Previous experiments have shown that when a pressure head exists across the aperture array there is an associated mass current oscillating at the Josephson frequency [3]. (ii) For a BCS-type superfluid, it is well known that  $\rho_s$  decreases with superfluid current [9–11]. Therefore the Josephson current oscillations will give rise to a *decremental* oscillation of  $\rho_s$ . (iii) The decrease in  $\rho_s$  is associated with the creation of quasiparticles within the aperture [12].

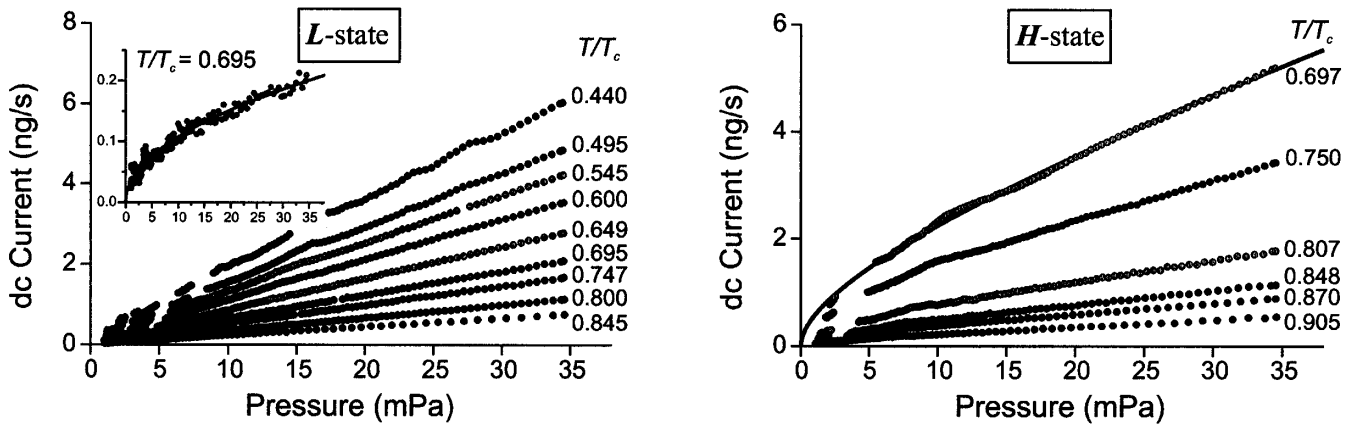


FIG. 1. The measured dc current is plotted as a function of the pressure across the weak link for both  $H$  and  $L$  states and critical currents below 25 ng/s. The gaps in the data are where the largest of the dc current enhancements (Fiske effect distortions [7]) have been removed for clarity of fit (some small distortions are still visible at low temperatures). For critical currents above  $\sim 25$  ng/s, the  $I$ - $P$  distortions become broad and are continuous throughout the accessible pressure range making a meaningful fit to (1) problematic. The solid line (for  $T/T_c = 0.697$  in the  $H$  state) is an example of a fit to (1). The inset (for  $T/T_c = 0.695$  in the  $L$  state) shows the  $\sqrt{P}$  character of the quasiparticle current,  $I_2$  (notice the small size of  $I_2$  for the  $L$  state so that the  $I$ - $P$  curves appear purely linear at first glance). To obtain this curve, a fit of the  $I$ - $P$  curve was made to (1) producing  $G_1$  and  $G_2$ . Then the quasiparticle current is given by  $I - G_1P$  and the solid line is given by  $I_2 = G_2\sqrt{P}$ .

(iv) Since, at mK temperatures, the quasiparticle mean free path is very large compared to the dimensions of the aperture, they will be ballistically swept away from the apertures by the local pressure gradient [13]. The resultant current is somewhat analogous to that in a photodiode wherein photons create electrons in the junction which are steadily removed by the electric field. (v) The average drift velocity of the quasiparticles,  $\langle v_n \rangle = \sqrt{2P/\rho}$ , is derived from energy considerations. This is the origin of the  $\sqrt{P}$  dependence. The associated dissipative quasiparticle current density is  $J_2 \equiv \langle \delta\rho_n \rangle \langle v_n \rangle$ , where  $\langle \delta\rho_n \rangle$  is the time-averaged density of the quasiparticles created during a Josephson period. For  $N$  apertures with individual cross-sectional area  $\sigma$ , the total current is then proportional to  $\sqrt{P}$  with proportionality constant given by

$$G_2 = \langle \delta\rho_n \rangle N \sigma \sqrt{\frac{2}{\rho}}. \quad (2)$$

Since  $\langle \delta\rho_n \rangle$  depends on the time variation of the supercurrent, the detailed shape of the current-phase relation  $I(\phi)$  produces different values of  $G_2$  for the  $H$  and  $L$  states [14]. Using existing predictions for the suppression of the

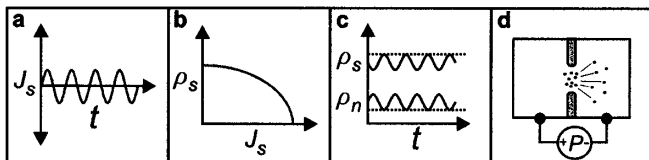


FIG. 2. Visualizing the creation of a quasiparticle current. (a) Josephson current oscillations in time. (b) The dependence of the superfluid density  $\rho_s$  as a function of the current density  $J_s$ . (c) The resultant *decremental* oscillations of  $\rho_s$  and the associated *incremental* oscillations in  $\rho_n$ . (d) Ballistic quasiparticles being swept away from an aperture by the local pressure gradient.

superfluid density with current density [9,10,15] and our experimental determination [4] of  $I(\phi)$ , we can generate [15] the values for  $\langle \delta\rho_n \rangle$  and from (2) predict  $G_2$  as a function of temperature. The solid line in Fig. 3 shows our predictions for  $G_2$  based on a weak coupling BCS treatment [10], valid for all temperatures. In Fig. 3 we also plot the measured values of  $G_2$  for both  $H$  and  $L$  states (notice the large difference between the values for  $G_2$  in each state).

These predicted curves are in remarkably good agreement with the data. In (2) we have adjusted the aperture area  $\sigma$  to get the best agreement with *both* sets of data ( $H$  and  $L$ ). This gives a *single* value  $\sigma = 1.4 \times 10^{-14}$  m<sup>2</sup>. Using effusion data we independently determined the aperture area to be  $\sigma = 1.36 \times 10^{-14}$  m<sup>2</sup>. Although the good quantitative agreement between our prediction and the experimental data is probably fortuitous, since we do not know the precise details of the superfluid behavior in the coherence length sized apertures, it does provide strong support for the ideas involved in deriving (2).

Our inspection of the published literature describing driven flow experiments shows  $\sqrt{P}$  features in the  $I$ - $P$  relation even when the dimensions of the orifices are large compared to the coherence length  $\xi$ . The  $I$ - $P$  curves obtained for long narrow pores [16] show a current roughly proportional to  $\sqrt{P}$  beyond a critical velocity. If the critical velocity for flow is determined by vortex line creation within the pore, subsequent pressure-driven flow will be associated with a saw-tooth oscillation of the superfluid velocity resulting from the periodic passage of  $2\pi$  vortices across the pore. A dc current given by (2) will be produced dependent on the amplitude of the velocity oscillation. Using a Landau-Ginzburg approximation [9] we have predicted these currents for  $B$ -phase superfluid  $^3\text{He}$  at 0 bar and we find they agree with experiment [16] within a factor of 2. We have also done a similar calculation for

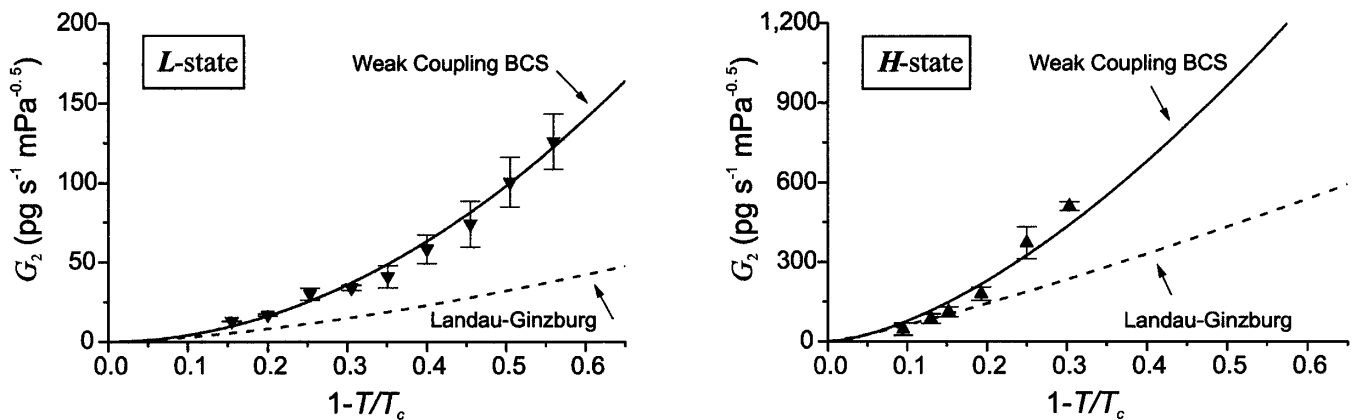


FIG. 3. The values for  $G_2$  are plotted for both the  $H$  state (up triangles) and  $L$  state (down triangles) as a function of  $(1 - T/T_c)$ . The dashed line shows our predictions for  $G_2$  using (2) based on a Landau-Ginzburg expansion of the free energy [9]. The solid line shows our predictions for  $G_2$  using (2) based on a weak coupling BCS treatment [10], valid for *all* temperatures less than  $T_c$ .

micron size holes in a thin window and have found consistent agreement with experiment [17].

We note that nonlinear  $I$ - $V$  features, which increase at lower temperature, have been observed in superconducting weak links (microbridges) [18,19]. Some of these features have been explained using dynamic models with assumptions somewhat similar to ours [12,20,21]. Microscopic theories based on Josephson oscillations of the energy gap have also been used to quantitatively describe nonlinear features in  $I$ - $V$  curves [22].

We now turn to the first term in (1). The existence of the linear conductance term,  $G_1$ , can be understood based on preexisting models as follows. Although the bulk fluid surrounding the weak link is  $^3\text{He-B}$ , within the confined dimensions of a coherence length sized aperture it is known from both theory [23] and experiments [24] that the order parameter of the  $B$  phase must distort to that of an anisotropic superfluid similar [25,26] to  $^3\text{He-A}$ .

An anisotropic superfluid is characterized by a unit vector field or  $\hat{\ell}$  texture, where  $\hat{\ell}$  points in the direction of the Cooper-pair angular momentum. When a chemical potential difference exists between two points in the  $A$  phase, if the superfluid is not accelerating,  $\hat{\ell}$  will exhibit precessional motion at the Josephson frequency [27–29]. Thus the entire texture within the aperture may be thought to precess at the Josephson frequency [30]. Because of the finite relaxation time of quasiparticles, motion of the texture is an inherently dissipative process with the orbital viscosity  $\mu_\ell$  as the relevant dissipative coefficient [31]. The power dissipated per unit volume is given [32] by  $\mu_\ell(\dot{\ell})^2$ .

We may estimate the dc current associated with orbital precession by equating the Ohmic power dissipation (current  $\times$  chemical potential difference) to the time averaged energy lost due to the precessing  $\hat{\ell}$  vector [33]:

$$\begin{aligned} \frac{IP}{\rho} &= \left\langle \mu_\ell \int (\dot{\ell})^2 d^3r \right\rangle \approx \beta \mu_\ell (\omega_J)^2 \int d^3r \\ &= \beta \mu_\ell \left( \frac{2m_3 P}{\rho \hbar} \right)^2 V_{\text{eff}}. \end{aligned} \quad (3)$$

Here the factor  $\beta$ , which is of order unity, represents an average over the spatial orientations of  $(\hat{\ell})^2$  and  $V_{\text{eff}}$  is the effective volume of the anisotropic phase region surrounding one aperture. Using the definition  $I_1 = G_1 P$  and (3), the conductance of  $N$  apertures is given by

$$G_1 = \beta N V_{\text{eff}} \frac{\mu_\ell}{\rho} \left( \frac{2m_3}{\hbar} \right)^2. \quad (4)$$

Notice that, in contrast to  $G_2$ , this expression is independent of the form of the current-phase relation of the weak link array and the temperature dependence comes from the orbital viscosity coefficient. (The effective size of the  $A$ -phase region should not vary strongly with temperature since the confining geometry alone stabilizes the state.) For small dimension passages one finds a similar expression [30] for  $G_1$  when starting with the superfluid equation of motion.

Using an expression [31,34] for  $\mu_\ell(T)$  (which is valid only near  $T_c$ ) and taking  $\beta = 1$ , we can compare the linear conductance given by (4) (near  $T_c$ ) with  $G_1$  determined by the fit of (1) to the data in Fig. 1. We can estimate  $V_{\text{eff}}$  in (4) to be given by the average aperture area ( $1.36 \times 10^{-14} \text{ m}^2$ ) times the sum of the membrane thickness (50 nm) plus a zero temperature coherence length (65 nm). This yields a volume of  $1.6 \times 10^{-21} \text{ m}^3$ . Figure 4 shows good agreement between (4) and the data for *both*  $H$  and  $L$  states, in the regime where  $\mu_\ell(T)$  is known, if  $V_{\text{eff}} = 1.4 \times 10^{-21} \text{ m}^3$ , rather close to our estimate. This agreement strongly supports the idea that orbital dissipation from precessing textures determines the linear conductance. At lower temperatures our measured values of  $G_1$  provide the first direct measure of  $\mu_\ell(T)$  in the regime where a theoretical expression does not yet exist.

In summary, we have measured the current-pressure characteristic for superfluid  $^3\text{He}$  forced through small apertures. We find that there are dissipative currents much larger than that due to the normal fluid background. We have quantitatively accounted for two dissipative shunt currents varying as  $\sqrt{P}$  and  $P$ . The  $\sqrt{P}$  term, which is

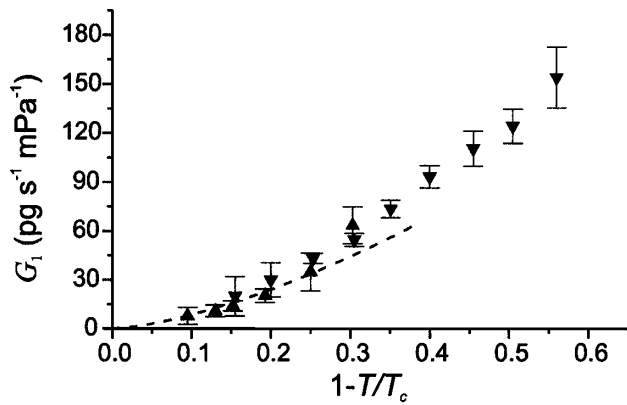


FIG. 4. The magnitude of  $G_1$  plotted as a function of  $(1 - T/T_c)$  for both the  $H$  state (up triangles) and the  $L$  state (down triangles). The dashed line was generated from (4) using the theoretical expression [31,34] for  $\mu_\ell(T)$  (valid near  $T_c$ ), taking  $\beta = 1$ , and the fit value  $V_{\text{eff}} = 1.4 \times 10^{-21} \text{ m}^3$ . The data agree very well with our prediction for both  $H$  and  $L$  states for temperatures near  $T_c$ . At lower temperatures our measured values of  $G_1$  provide the first direct measure of  $\mu_\ell(T)$  in a regime where a theoretical expression does not exist.

explained by a new theory involving flow induced creation of quasiparticles has led us to an explanation of previously unexplained experimental results on the forced flow of  $^3\text{He}$  through tubes and large apertures. The linear term is consistent with orbital precession in a chemical potential gradient.

It is a pleasure to acknowledge useful discussions with G. Volovik, N. Kopnin, T. Ho, D-H. Lee, A. Fetter, R.L. Kautz, and J. Hook. S. Pereversev, Yu. Mukharsky, J. Steinhauer, A. Loshak, and S. Backhaus contributed to the early stages of this work. This research was supported in part by grants from NSF, NASA, ONR, and NEDO.

\*Permanent address: Physics Department, University of Trento, I-38050 Povo, Trento, Italy.

- [1] P.W. Anderson, *Rev. Mod. Phys.* **38**, 298 (1966).
- [2] See, for example, Refs. [12,20,21].
- [3] S.V. Pereverzev *et al.*, *Nature (London)* **388**, 449 (1997).
- [4] A. Marchenkov *et al.*, *Phys. Rev. Lett.* **83**, 3860 (1999).
- [5] S. Backhaus *et al.*, *Science* **278**, 1435 (1997).
- [6] S. Backhaus and R. Packard, in *Proceedings of the 21st International Conference on Low Temperature Physics [Czech. J. Phys.* **46**, 2743 (1996)].
- [7] R.W. Simmonds *et al.*, *Phys. Rev. Lett.* **81**, 1247 (1998).
- [8] J.K. Viljas and E.V. Thuneberg, *Phys. Rev. Lett.* **83**, 3868 (1999).
- [9] A.L. Fetter, in *Quantum Statistics and the Many Body Problem*, edited by S.B. Trickey, W.P. Kirk, and J.W. Duffy (Plenum Press, New York, 1975), p. 127.
- [10] D. Vollhardt, K. Maki, and N. Schopohl, *J. Low Temp. Phys.* **39**, 79 (1980).
- [11] H. Kleinert, *J. Low Temp. Phys.* **39**, 451 (1980).
- [12] B.S. Deaver, Jr., R.D. Sandell, and D.A. Vincent, *Phys. Lett.* **46A**, 411 (1974).
- [13] P.G. de Gennes, *Superconductivity of Metals and Alloys* (Addison-Wesley, Redwood City, CA, 1989).
- [14] The time average of the quasiparticle density is  $\langle \delta \rho_n \rangle = \rho_s(0, T) - (1/\tau) \int_0^\tau \rho_s[J(t), T] dt$ , where  $J(t) = I[\phi(t)]/N\sigma$ . The phase has a time dependence given by the ac Josephson relation,  $\phi(t) = (2m_3P/\hbar\rho)t = \omega_J t$ . This allows us to perform the time average by averaging over the quantum phase  $\phi$ ,  $\langle \delta \rho_n \rangle = \rho_s(0, T) - (1/2\pi) \int_0^{2\pi} \rho_s[I(\phi), T] d\phi$ . Using our measurements of  $I(\phi)$  at a number of temperatures we numerically calculate  $\langle \delta \rho_n \rangle$ .
- [15] To calculate  $\langle \delta \rho_n \rangle$  it is necessary to have the relation between superfluid mass density and current density [i.e.,  $\rho_s(J_s)$ ]. In the Landau-Ginzburg limit [9] we could derive an analytic form of this function. This result is valid only near  $T_c$ . To obtain  $\rho_s(J_s, T)$  for all temperatures we took theoretical curves [10] for  $\rho_s(\nu_s)$  and numerically generated curves for  $\rho_s(J_s)$  for all the predicted temperatures. We can use predictions for the equilibrium state because the Josephson period is much greater than the quasiparticle collision time.
- [16] M.T. Manninen and J.P. Pekola, *J. Low Temp. Phys.* **52**, 497 (1983).
- [17] J. Steinhauer *et al.*, in *Proceedings of the 20th International Conference on Low Temperature Physics* (North-Holland, Eugene, OR, 1994), Vols. 194–196, p. 767.
- [18] C.H. Arrington and B.S. Deaver, Jr., *Appl. Phys. Lett.* **26**, 204 (1975).
- [19] M. Octavio, W.J. Skocpol, and M. Tinkam, *Phys. Rev. B* **17**, 159 (1978).
- [20] B.S. Deaver, Jr., R. Rifkin, and R.D. Sandell, *J. Low Temp. Phys.* **25**, 409 (1976).
- [21] B.S. Deaver, Jr., B.G. Boone, and R. Rifkin, *Phys. Lett.* **57A**, 186 (1976).
- [22] A. Schmid, G. Schön, and M. Tinkham, *Phys. Rev. B* **21**, 5076 (1980).
- [23] U. Ambegaokar, P.G. de Gennes, and D. Rainer, *Phys. Rev. A* **9**, 2676 (1974).
- [24] M.R. Freeman *et al.*, *Phys. Rev. Lett.* **60**, 596 (1988).
- [25] Y.-H. Li and T.L. Ho, *Phys. Rev. B* **38**, 2362 (1988).
- [26] A.L. Fetter and S. Ullah, *J. Low Temp. Phys.* **70**, 515 (1988).
- [27] H.E. Hall and J.R. Hook, *J. Phys. C* **10**, L91 (1977).
- [28] T.L. Ho, *Phys. Rev. Lett.* **41**, 1473 (1978).
- [29] G.E. Volovik, *J. Exp. Theor. Phys. Lett.* **27**, 573 (1978).
- [30] H.E. Hall and J.R. Hook, *Hydrodynamics of Superfluid  $^3\text{He}$*  (North-Holland, Amsterdam, 1986).
- [31] M.C. Cross and P.W. Anderson, in *Proceedings of the 14th International Conference on Low Temperature Physics, Ontaniemi, Finland, 1975*, edited by M. Krusius and M. Vuorio (North-Holland, Amsterdam, Oxford, 1975), Vol. 1, p. 29.
- [32] M.C. Cross, in *Quantum Fluids and Solids, Sanibel Island, FL, 1983*, edited by E. Dwight Adams and G.G. Ihas (American Institute of Physics, New York, 1983), Vol. 103, p. 325.
- [33] A.L. Fetter, *J. Low Temp. Phys.* **70**, 499 (1988).
- [34] C.J. Pethick and H. Smith, *Phys. Rev. Lett.* **37**, 226 (1976).